

---

## ***Evaluating the impact of the construction of the New Assiut Barrage on the groundwater level***

*Mohammed khoudary<sup>1\*</sup>, Shenouda Ghaly<sup>2</sup>, Kamal Ali<sup>1</sup>, Gamal Abozaid<sup>3</sup>, and Hickmat Hossen<sup>1</sup>*

*<sup>1</sup> Civil Engineering Department, Aswan University, Aswan, Egypt*

*<sup>2</sup> Arab Academy for Science Technology & Maritime Transport, Aswan, Egypt*

*<sup>3</sup> Civil Engineering Department, Assiut University, Assiut, Egypt*

### **ABSTRACT**

The construction of new barrages increases the levels of groundwater, which affects the foundations of structures and agricultural land in those areas. It was therefore necessary to study the effect of the construction of New Assiut Barrage on increasing the levels of groundwater in the city of Assiut. New Assiut Barrage (NAB) is located in the city of Assiut, which was constructed about 400 meters north of the location of Old Assiut Barrage. It is expected that after the operation, an increase in surface water levels will occur in the upstream of barrage (next to the Al-Walidiyah district) and an increase in surface water levels in the downstream along the northern bank of Assiut city. All this in turn increases the levels of groundwater and also submerges part of the northern bank of city. This study is based on Finite Difference method (FDM) and Geographical Information Systems (GIS) to produce two types of layers. The first layer has the values of groundwater levels for the entire study area, the second layer is a map of the terrain of the earth. Through the analysis of the two layers, can be determined the places of appearance of groundwater above the surface of the earth, and the amount of immersion in the northern banks.

**Keywords:** New Assiut Barrage (NAB), Finite Difference Method (FDM), GIS, Groundwater level (GWL).

### **1 INTRODUCTION**

The Construction of NAB was aimed at improving the irrigation situation in the central Egypt region in five governorates (Giza, Fayoum, Beni Suef, Menia, and Assiut) to serve 650,000 feddans. As well as improving river navigation in the Nile River using the latest global control systems; to control the flow and water level, as well as the establishment of a clean electricity production plant. The project also aimed to create a new traffic hub in Assiut, thus contributing to the cultural and environmental transition of the governorate. The construction of the New Assiut Barrage (NAB) induces the formation of a backwater curve on the upstream side, resulting in an

---

Corresponding author E-mail: [mohammed.khoudary@aswu.edu.eg](mailto:mohammed.khoudary@aswu.edu.eg)

Received October 15, 2023, Revised November 24, 2023 accepted November 26, 2023.

(ASWJST 2023/ printed ISSN: 2735-3087 and on-line ISSN: 2735-3095) <https://journals.aswu.edu.eg/stjournal>

elevation of surface water levels. This increase in surface water levels gradually permeates the soil, causing a rise in groundwater levels (GWL). Monitoring GWL changes due to human-made structures, especially embankments, holds significant importance in Egypt's comprehensive water resources management plan [1]. Elevated GWL can adversely affect building foundations [2,3,4]. Additionally, [5] delves into the implications of groundwater on soil quality, crop production, and its utilization in Egyptian agriculture. Groundwater modeling employs various numerical techniques for GWL calculations, including the finite difference method (FDM), finite volume method (FVM), and finite element method (FEM). The finite difference model (FD model) and geographic information systems (GIS) are extensively employed for monitoring groundwater fluctuations [6]. FDM has been applied in GWL modeling by numerous researchers [7,8,9,10,11], and several Egyptian scholars have contributed research on the impact of barrages in Egypt and GWL fluctuations [12,13,14,15,16,17]. The utilization of GIS in groundwater research is on the rise, covering aspects such as groundwater potential [18], vulnerability assessment [19], modeling [20, 21], and management [22]. The main objective of this study is to monitor changes in GWL by predicting its spatial distribution in the study area post the implementation of the New Assiut Barrage (NAB) and to observe the resulting effects on the region.

## 2 FINITE DIFFERENCES

FDM is considered as the most applicable and easily understood methods of obtaining numerical solutions to steady and unsteady groundwater flow problems [23]. The Finite Difference Method offers several advantages in groundwater flow simulations. Firstly, it is a comprehensible method that can be easily understood and implemented by researchers and practitioners in the field [24]. Furthermore, the Finite Difference Method is known for its accuracy and stability, providing reliable numerical solutions for groundwater flow problems [25]. Additionally, the Finite Difference Method can handle heterogeneous aquifers effectively [26], as it does not rely on post-processing techniques for determining flux. Instead, it directly calculates the flux at each node using Darcy's Law. Therefore, for complex areas with heterogeneous aquifers, the Finite Difference Method is the preferred numerical technique for solving groundwater mathematical models, especially when accurate flux calculations are required [27]. The Finite Difference Method operates by superimposing a finite difference grid of nodes onto the solution domain. Each node in the grid is assigned a unique global identification number, which also extends to its adjacent nodes. This numerical technique estimates the dependent variable through a finite-degree polynomial, with coefficients expressed as functions of the unknown values of the dependent variable at neighboring nodes. This polynomial is crucial in establishing an algebraic approximation for the partial differential equation associated with each internal node, as well as approximating the boundary conditions for each node on or near the boundary of the solution domain [28].

Laplace's equation is used in the finite difference approximation operation for such a mesh is given by aquifer, we get a single second-order partial differential equation [29]:

$$\frac{\partial^2 h}{\partial^2 x} + \frac{\partial^2 h}{\partial^2 y} + \frac{\partial^2 h}{\partial^2 z} = 0 \quad (1)$$

When  $x,y,z$  directions and  $h$  is head of groundwater.

This is Laplace's equation, which describes the flow of groundwater under steady-state conditions within an isotropic and homogeneous aquifer. This equation essentially asserts that the combined

partial derivatives of head ( $h$ ) concerning the  $x$ ,  $y$ , and  $z$  axes sum up to zero (in a two-dimensional context). To solve Laplace's equation, it is necessary to establish boundary conditions in the study area, including Dirichlet conditions and Neumann conditions [30]. Given that groundwater flow occurs in two dimensions, Laplace's equation can be simplified to:

$$\frac{\partial^2 h}{\partial^2 x} + \frac{\partial^2 h}{\partial^2 y} = 0 \quad (2)$$

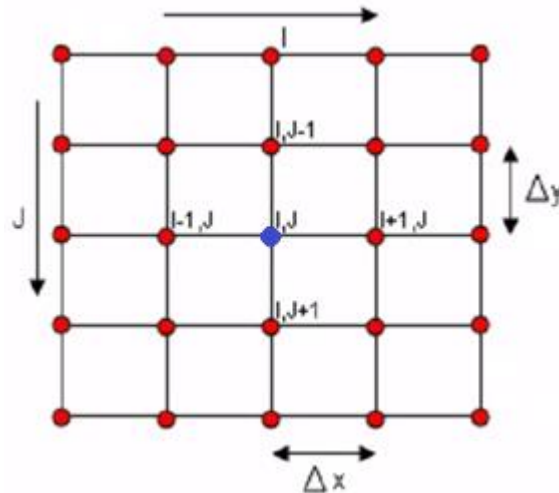


Fig. 1. Finite difference grid of nodes.

As illustrated in Fig. 1, considered a grid of nodes arranged in  $i$  columns and  $j$  rows. These nodes are separated by horizontal intervals ( $\Delta x$ ) and vertical intervals ( $\Delta y$ ), the head at node  $i, j$  is  $h_{ij}$ , discretization of the equation terms as follows:

$$\frac{\partial^2 h}{\partial^2 x} = \frac{h_{i-1,j} - 2h_{i,j} + h_{i+1,j}}{(\Delta x)^2}, \quad \frac{\partial^2 h}{\partial^2 y} = \frac{h_{i,j-1} - 2h_{i,j} + h_{i,j+1}}{(\Delta y)^2} \quad (3)$$

Generally, in case of:

$$\Delta x_{i \rightarrow i-1} \neq \Delta x_{i \rightarrow i+1} \text{ and } \Delta y_{j \rightarrow j-1} \neq \Delta y_{j \rightarrow j+1}$$

$$\frac{h_{i-1,j} - h_{i,j}}{(\Delta x_{i \rightarrow i-1})^2} + \frac{h_{i+1,j} - h_{i,j}}{(\Delta x_{i \rightarrow i+1})^2} + \frac{h_{i,j-1} - h_{i,j}}{(\Delta y_{j \rightarrow j-1})^2} + \frac{h_{i,j+1} - h_{i,j}}{(\Delta y_{j \rightarrow j+1})^2} = 0 \quad (4)$$

In case of equal grid:

$$\Delta x_{i \rightarrow i-1} = \Delta x_{i \rightarrow i+1} \text{ and } \Delta y_{j \rightarrow j-1} = \Delta y_{j \rightarrow j+1}$$

$$\frac{h_{i-1,j} - 2h_{i,j} + h_{i+1,j}}{(\Delta x)^2} + \frac{h_{i,j-1} - 2h_{i,j} + h_{i,j+1}}{(\Delta y)^2} = 0 \quad (5)$$

If,  $\Delta x = \Delta y$

$$h_{i-1,j} + h_{i+1,j} + h_{i,j-1} + h_{i,j+1} - 4h_{ij} = 0 \quad (6)$$

The equations described above are commonly employed in finite difference solutions for steady-state flow problems. They are iteratively applied using a Laplacian operator to calculate head values at each node within the grid [31].

- **Configuration of The Mesh**

Based on the previous equations and the area shown in Fig. (2a) (for example), the domain was represented by the large number of squares or a network of rectangles, as shown in (Fig. 2b,c). The nodes are positioned so that, achieve a compatibility with the boundary conditions of the region, as well as good simulation of domain give a high accuracy result. In general vision, this is the system mostly used in groundwater modeling programs which depend on FDM [32].

Increasing the number of squares in the grid leads to an increase in the number of equations. This affects the increased time spent in the formation of equations and also to find solutions. Also, the use of networks with unequal units or non-identical rectangle, has a difficulty in the installation and has a different input in their equations to each node (depending on their dimensions).

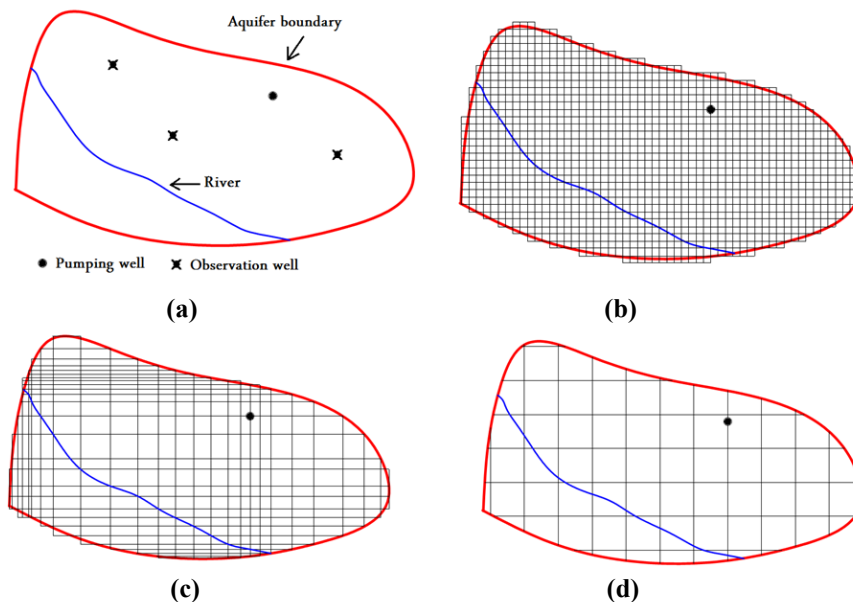


**Fig. 2.** (a) Example of an illustration map containing the boundary conditions, (b) FDM with mesh of equal squares, (c) FDM with mesh of unequal rectangles and (d) Proposed system to FDM in this thesis.

In this study, a different modeling system is proposed as in Fig. (2d), by using composite system of equal square units in internal area, except for the edges surrounding the studied area or next to the internal phenomena, to this case, the squares are cut out, and also use Eq. (4). In the case of an internal phenomena such as the river, the study area is divided into two parts, each part has its own equations. The proposed system reduces the number of equations, has flexibility in the model configuration pattern and gives a good match with the domain, thus reducing the time to create, solve the model and give good expected accuracy.

### 3 STUDY AREA

The study area is situated in Assiut Governorate, at coordinates 27° N and 30° E, covering an area of approximately 13.3 square kilometers. It is bounded to the north, west, and east by the Nile River, and to the south by Al-Ibrahimiya Canal. Al-Waleediyah Canal runs through the area, passing near Al-Walidiyah district. Notably, the New Assiut Barrage (NAB) is located to the east of the study area, approximately 400 meters north of the Old Assiut Barrage. The Al-Walidiyah district is densely populated and contains significant structures, making it particularly susceptible to alterations in surface water levels both upstream (U.S) and downstream (D.S) of the NAB, (see Fig.3a). The study area is located in the Nile Valley aquifer region [33], which means that the Nile River and the canals near it, are considered the main recharge for groundwater, and the greatest influence on it, especially during the summer months, due to the scarcity of rain at this time. The soil in the study area is located in the Nile Silt Zone as cleared in Fig.3b [34,35], and there are no significant differences in its morphological and geological properties [36,37], so the soil of the study area is considered homogeneous and isotropic.

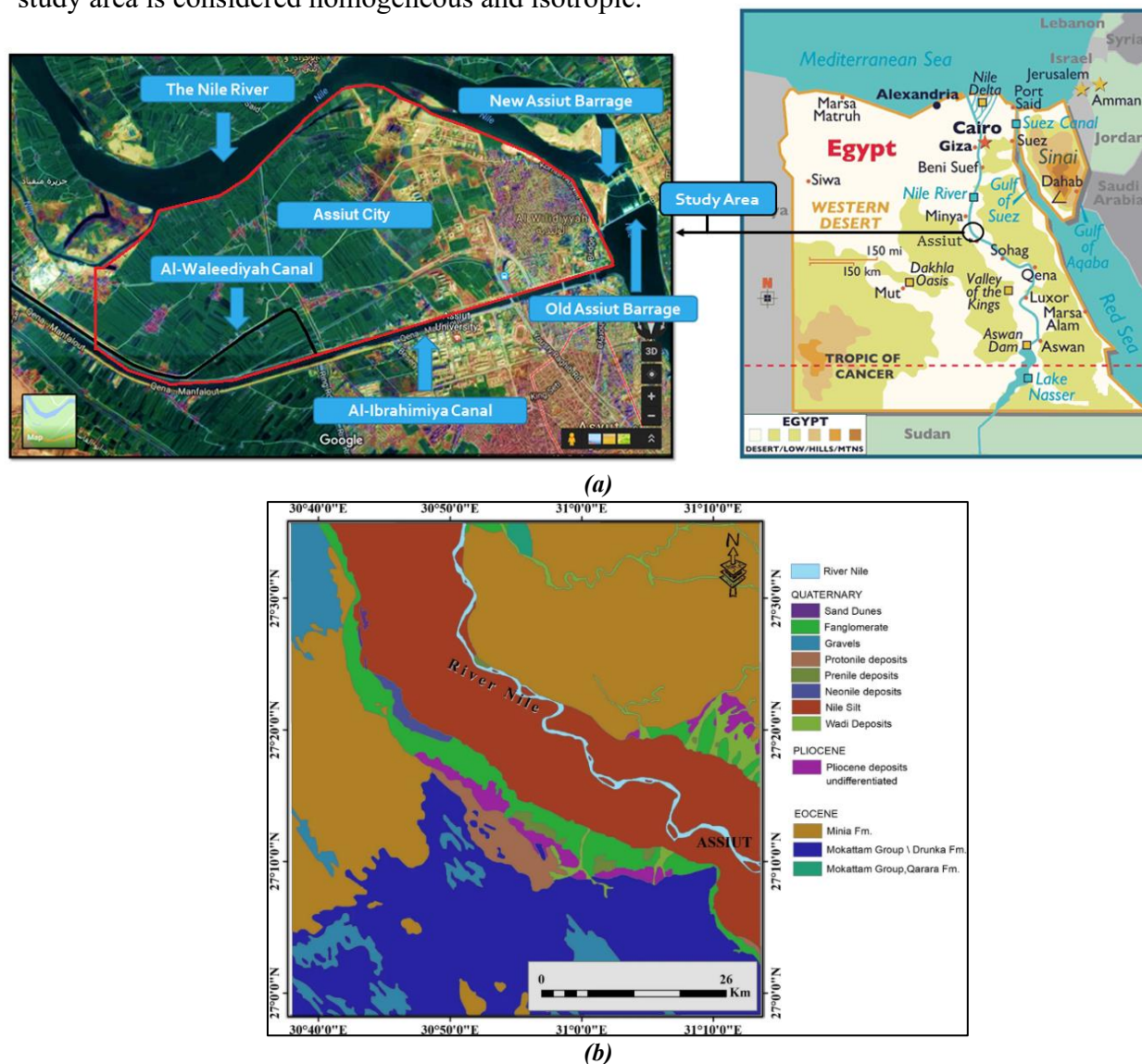


Fig. 3. (a) Map of the study area with the boundary conditions. (b) Lithologic map of the studied Assiut area [38].

#### 4 BOUNDARY CONDITIONS AND HYDROLOGICAL DATA

In this study, hydrological data were collected, encompassing groundwater levels (GWL) and surface water levels in the boundary conditions, both before and after the construction of the New Assiut Barrage (NAB). The Ministry of Irrigation in Assiut Governorate provided data on surface water levels in all boundary conditions from 2010 to 2017, as detailed in Table 1 and Table 2. Additionally, information about piezometer locations and their respective readings during the same period was made available, as depicted in Fig.4 and Table 3. These datasets will be instrumental in calibrating the model's outcomes at a later stage.

The hydrological boundary conditions and phenomena were translated into a series of points, each defined by its spatial coordinates (X, Y) denoting location and (Z) representing the water level (either surface water or groundwater). These spatial coordinates (X, Y, Z) for each point were employed to establish boundary conditions on the study area's map, forming the basis for creating 3-D elements and simulating the study area within the finite difference model (FD model).

*Table 1. Surface water levels in Boundary Conditions before NAB operation.*

| Year | Day<br>(Max/Min) | Nile River<br>(Old Assiut Barrage) |                |                | AL-Ibrahimiya<br>Canal<br>(Intake) |                |                | Al-Waleediyah<br>Canal<br>(Intake) |                |                |
|------|------------------|------------------------------------|----------------|----------------|------------------------------------|----------------|----------------|------------------------------------|----------------|----------------|
|      |                  | U.S.W.L<br>(m)                     | D.S.W.L<br>(m) | Slope<br>cm/km | U.S.W.L<br>(m)                     | D.S.W.L<br>(m) | Slope<br>cm/km | U.S.W.L<br>(m)                     | D.S.W.L<br>(m) | Slope<br>cm/km |
| 2010 | 1/8              | 50.31                              | 47.0           | 4              | 50.24                              | 49.54          | 6              | 51.35                              | 51.25          | 8              |
|      | 1/12             | 48.60                              | 44.96          | 5              | 47.97                              | 47.91          | 8              | 51.35                              | 51.10          | 10             |
| 2011 | 1/8              | 49.80                              | 47.15          | 4              | 49.71                              | 49.69          | 6              | 51.20                              | 51.10          | 8              |
|      | 1/12             | 48.30                              | 44.94          | 5              | 48.23                              | 48.07          | 8              | 51.50                              | 51.40          | 10             |
| 2012 | 1/8              | 49.80                              | 47.18          | 4              | 49.73                              | 49.68          | 6              | 51.30                              | 51.25          | 8              |
|      | 1/12             | 48.33                              | 45.12          | 5              | 48.26                              | 48.19          | 8              | 51.35                              | 51.20          | 10             |
| 2013 | 1/8              | 49.88                              | 47.29          | 4              | 49.81                              | 49.65          | 6              | 51.40                              | 51.35          | 8              |
|      | 1/12             | 48.22                              | 44.94          | 5              | 48.15                              | 48.09          | 8              | 51.40                              | 51.30          | 10             |
| 2014 | 1/8              | 49.86                              | 47.35          | 4              | 49.79                              | 49.73          | 6              | 51.30                              | 51.20          | 8              |
|      | 1/12             | 48.04                              | 44.80          | 5              | 47.97                              | 47.64          | 8              | 51.35                              | 51.15          | 10             |
| 2015 | 1/8              | 50.55                              | 47.42          | 4              | 50.48                              | 49.75          | 6              | 51.60                              | 51.40          | 8              |
|      | 1/12             | 48.40                              | 44.95          | 5              | 48.33                              | 47.94          | 8              | 51.40                              | 51.25          | 10             |
| 2016 | 1/8              | 49.97                              | 47.32          | 4              | 49.90                              | 49.70          | 6              | 51.25                              | 51.10          | 8              |
|      | 1/12             | 48.50                              | 45.10          | 5              | 48.43                              | 48.00          | 8              | 51.50                              | 51.25          | 10             |
| 2017 | 1/8              | 50.31                              | 47.30          | 4              | 50.24                              | 49.65          | 6              | 51.25                              | 51.10          | 8              |
|      | 1/12             | 49.20                              | 44.82          | 5              | 49.17                              | 47.71          | 8              | 50.60                              | 50.30          | 10             |

*Table 2. Surface water levels in Boundary Conditions after NAB operation (max case).*

| Max<br>case | Nile River<br>(New Assiut Barrage) |                |                | AL-Ibrahimiya Canal<br>(Intake) |                |                | Al-Waleediyah Canal<br>(Intake) |                |                |
|-------------|------------------------------------|----------------|----------------|---------------------------------|----------------|----------------|---------------------------------|----------------|----------------|
|             | U.S.W.L<br>(m)                     | D.S.W.L<br>(m) | Slope<br>cm/km | U.S.W.L<br>(m)                  | D.S.W.L<br>(m) | Slope<br>cm/km | U.S.W.L<br>(m)                  | D.S.W.L<br>(m) | Slope<br>cm/km |
|             | 51.13                              | 48.7           | 4              | 50.75                           | 49.8           | 6              | 51.60                           | 51.50          | 8              |

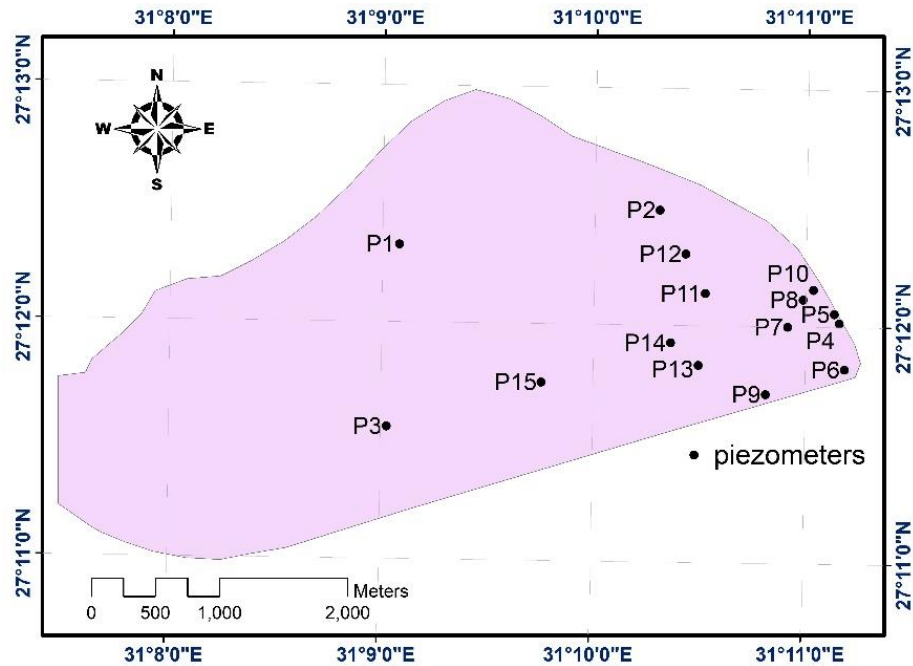


*Fig. 4. Map of Piezometers locations in Study Area.*

*Table 2. Coordinates of Piezometers.*

| <b>Piezometer ID</b> | <b>X (UTM)</b> | <b>Y (UTM)</b> | <b>Earth Levels (m)</b> |
|----------------------|----------------|----------------|-------------------------|
| P1                   | 316901.41      | 3010541.5      | 51.2                    |
| P2                   | 318932.21      | 3010803.75     | 53.68                   |
| P3                   | 316799.06      | 3009122.02     | 52.84                   |
| P4                   | 320327.41      | 3009916.5      | 54.68                   |
| P5                   | 320289.41      | 3009988.5      | 54.21                   |
| P6                   | 320367.96      | 3009557.74     | 54.32                   |
| P7                   | 319925.46      | 3009892.2      | 52.31                   |
| P8                   | 320046.6       | 3010103.11     | 53.36                   |
| P9                   | 319750.75      | 3009365.84     | 53.07                   |
| P10                  | 320126.82      | 3010177.33     | 54.5                    |
| P11                  | 319283.64      | 3010154.35     | 52.03                   |
| P12                  | 319132.18      | 3010461.57     | 51.36                   |
| P13                  | 319227.88      | 3009593.99     | 52.41                   |
| P14                  | 319013.41      | 3009770.5      | 53.2                    |
| P15                  | 318004.22      | 3009463.92     | 53.16                   |

Satellite images from the ASTRA satellite were harnessed to generate a corrected topographical layer for the study area, illustrated in Fig.5. This layer, in conjunction with the obtained GWL from the model, underwent processing through the ArcGIS software. The outcome was the creation of a new layer that identifies the specific locations where groundwater emerges above the land's surface within the study area. Furthermore, this process aimed to guarantee precise alignment between the

boundary condition locations in the selected model and their corresponding positions on the corrected terrain map. This alignment enhances the accuracy of the model's results.

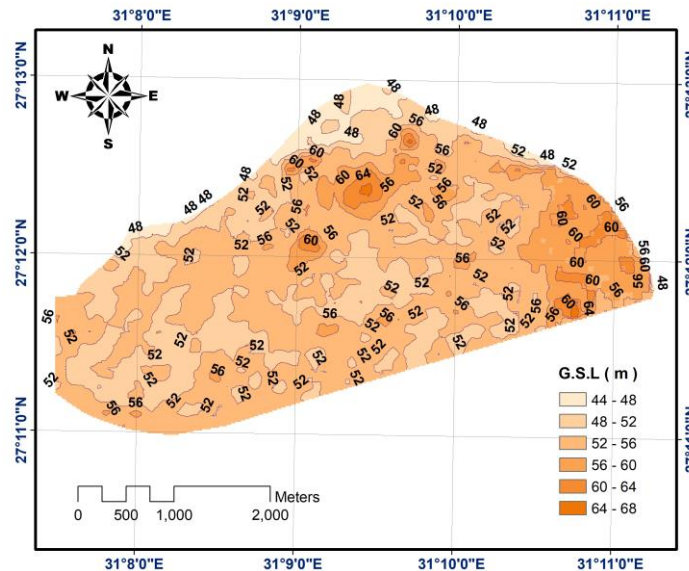


*Fig. 5. Map of the study area topography.*

## 5 MODEL PREPARATION

The preparation of the FD (Finite Difference) model involved a series of steps as follows (see Fig. 6):

- *Setting Boundary Conditions:* The initial step included defining the boundary conditions of the model.
- *Creating a Node Map:* A map of the study area is generated, incorporating a grid of nodes. This map was created using AutoCAD and ArcGIS software. To conserve time and effort for users of the proposed mesh method while achieving acceptable accuracy and compatibility with the characteristics and phenomena of the study area, intervals in both the X and Y directions between nodes are chosen at 250 meters. This decision was made after making a trial and error with many values of spacing, aiming to optimize efficiency. However, nodes close to the outer borders and boundary conditions are determined based on the study area map, as depicted in Fig.6.
- *Equation Assignment:* Each node was assigned an appropriate equation based on the specific conditions, as previously outlined. These equations were solved using Microsoft Excel software.
- *Model Calibration and Verification:* This step involved the calibration and verification of the model. To ensure model accuracy, data from the years 2010 to 2016, before the operation of the New Assiut Barrage (NAB), were employed. After calibration, the model was used to predict groundwater level (GWL) changes following the operation of NAB, facilitating the detection of variations in GWL.

To represent and solve the equations, a program is created by the Excel software, which contains all equations for each point in the grid. A simple program interface is created, which start up through the water level in upstream, downstream and the longitudinal slope of all boundary

conditions, from these initial data, surface water levels are calculated for all points that located on the boundary conditions. The program contains the equations for the other points (that have unknown value) in an array, so that when entering the initial values, the program calculates the values for each point. The program produces, interprets and synthesizes other grid points using the direct method, ultimately producing groundwater values for all points of the region and their locations.

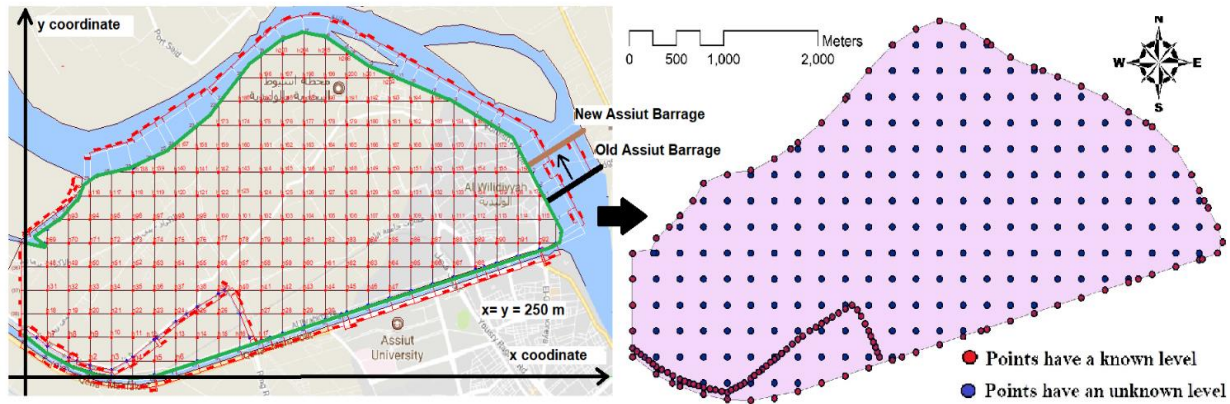


Fig. 6. Map of model's mesh.

In the ArcGIS program, two layers were created: one representing GWL based on the obtained model results and another indicating ground levels. An analysis was performed on these two layers to generate a third layer, which identifies the inundated locations along the banks and the areas where groundwater emerges within the study area (see Fig.7).

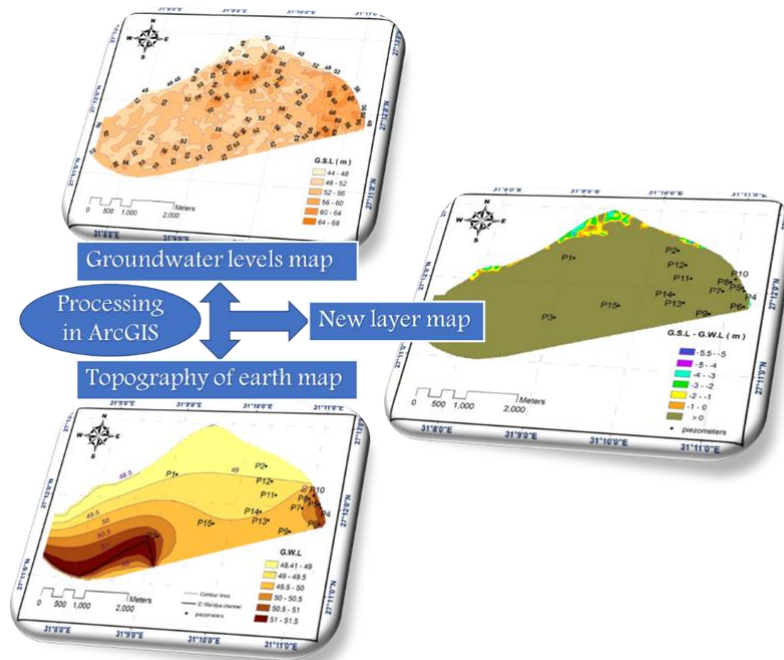


Fig. 7: Processing of two layer in ArcGIS program.

## 6 MODEL CALIBRATION AND VERIFICATION

The FD model underwent calibration and verification to ensure its accuracy:

- *Calibration stage:* The model was initially calibrated using data collected before the operation of the New Assiut Barrage (NAB). During this phase, the model's predictions were compared with observed groundwater level (GWL) data from selected piezometers. The calibration process revealed that there was a notable agreement between the estimated and observed GWL. The average correlation coefficient reached approximately 95.6%, and the average root mean square error (RMSE) was around 10.37%. At this stage, equations were established between the estimated values calculated from the model and the observed values, to be subsequently utilized in the verification and prediction phase, without the need for boundary condition adjustments.
- *Verification stage:* To further assess the model's performance, the year 2017 was used as the verification period. As depicted in Fig.8, the verification results demonstrated good validity. The correlation coefficient for this phase was approximately 0.987.

These calibration and verification phases ensured that the FD model could reliably predict GWL changes and provided accurate results for the study area.

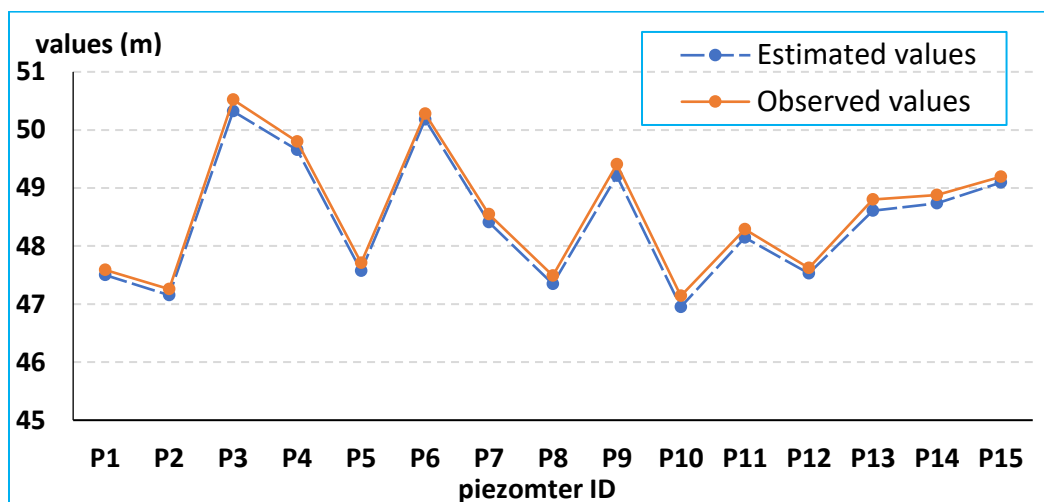


Fig. 8. Chart of calculated and observed values of piezometers (year 2017).

## 7 RESULT AND DISCUSSION

Fig. 9 shows the spatial distribution map of GWL estimated for the study area before and after the operation of NAB barrage at the maximum water level boundary conditions, while the map in Figure 9a shows the maximum groundwater levels for all study years before the operation of the NAB, which was in the year 2015, Figure 9b illustrates the GWL distribution after the operation of the NAB, based on forecasting. It represents the maximum case scenario after the barrage's operation. Figure 9 clearly shows the average groundwater rise of approximately 1.5 meters in each study area.

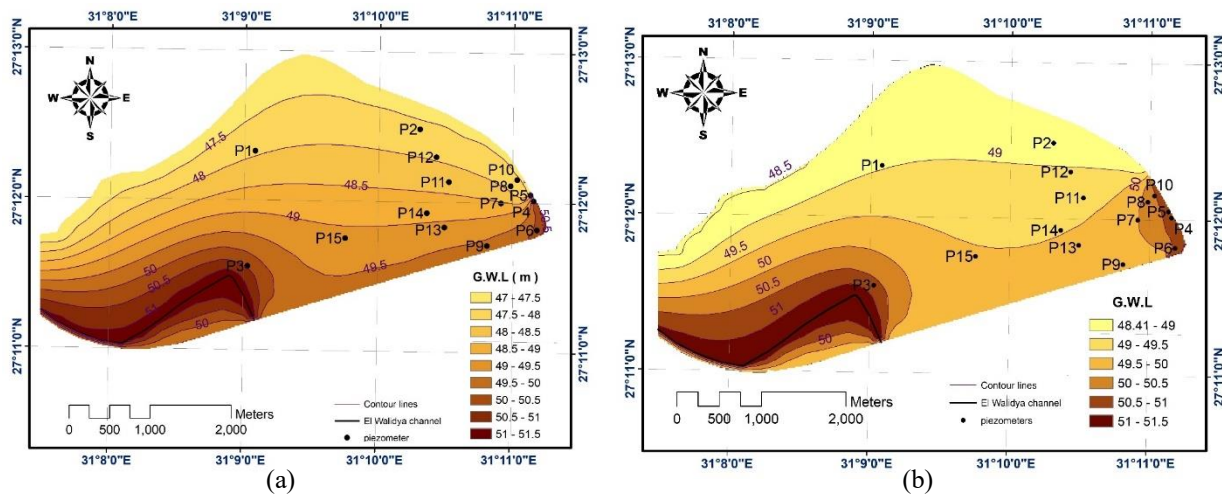


Fig. 9. (a) Spatial distribution map of GWL for study for year 2015 (August). (b) Spatial distribution map of GWL for study after barrage operation (max operation case).

Fig.10 presents a map created by subtracting GWL layer from the Ground Levels layer before and after the operation of the NAB using the ArcGIS program. This map effectively highlights the areas where groundwater appearance or where immersion occurs within the study area. In Fig. 10b, post-NAB operation, it's evident that the northern bank, adjacent to the Nile River, has experienced immersion. This immersion covers an area of 240 Feddan, which represents approximately 7.6% of the total study area. The immersion area extends over a total length of 4.25 kilometers, with the maximum immersion reaching about 5.5 meters. Comparatively, in the year 2015 (Fig. 10a), before the NAB operation, the immersion area along the banks was smaller, encompassing 168.3 Feddan, stretching over 2.91 kilometers, and the maximum immersion reached approximately 4.5 meters. These findings indicate a noticeable increase in the proportion of areas prone to immersion after the NAB's operation, marking a 50% average increase in the areas susceptible to immersion compared to pre-operation years. Additionally, there is an average 48% increase in the total length of banks exposed to immersion, considering the average across all pre-operation years. Importantly, the results reveal that groundwater does not appear at the Earth's surface within the study area's interior, specifically in Al-Waleediyah district.

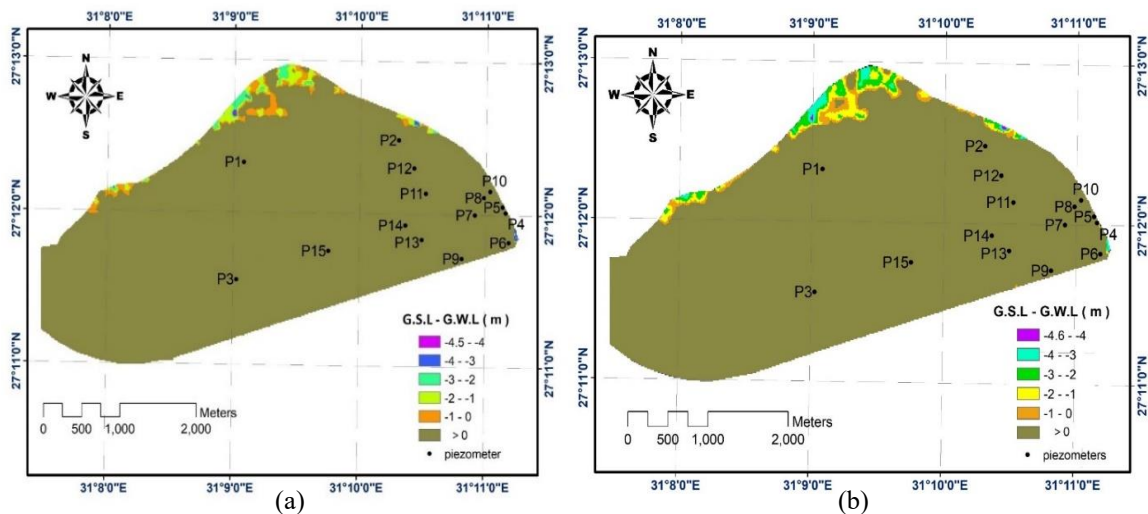


Fig. 10. (a) Spatial distribution map of immersion area for study before barrage operation in 2015, (b) Spatial distribution map of immersion area for study after barrage operation (max operation case).

Upon comparing the map of immersion areas on the banks of the study area with maps depicting the distribution of residential blocks, it is evident that there is no visible damage or the appearance of groundwater in these residential zones. However, there is an industrial area situated to the north of the study area, specifically at coordinates (317751.00 E and 3011590.31 N), as indicated by a circular marker in Fig. 11b. This industrial zone is anticipated to be submerged, due to the operation of the New Assiut Barrage in the maximum case scenario, as illustrated in Fig.11c.

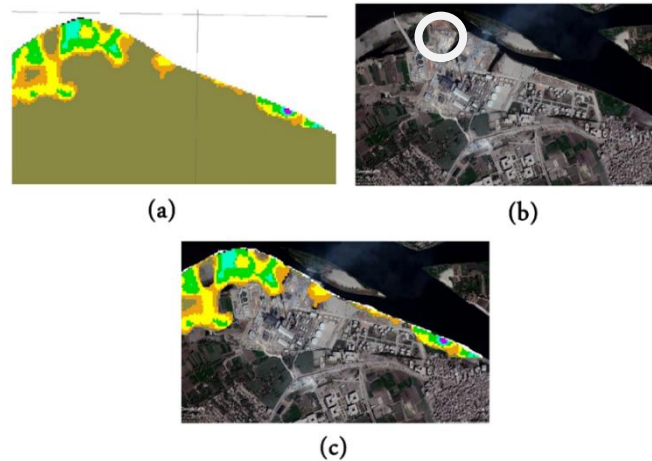


Fig. 11. (a) Part of the immersion map of the North bank in Fig. 10., (b) residential blocs distribution map [39], (c) overlapping image of two maps together.

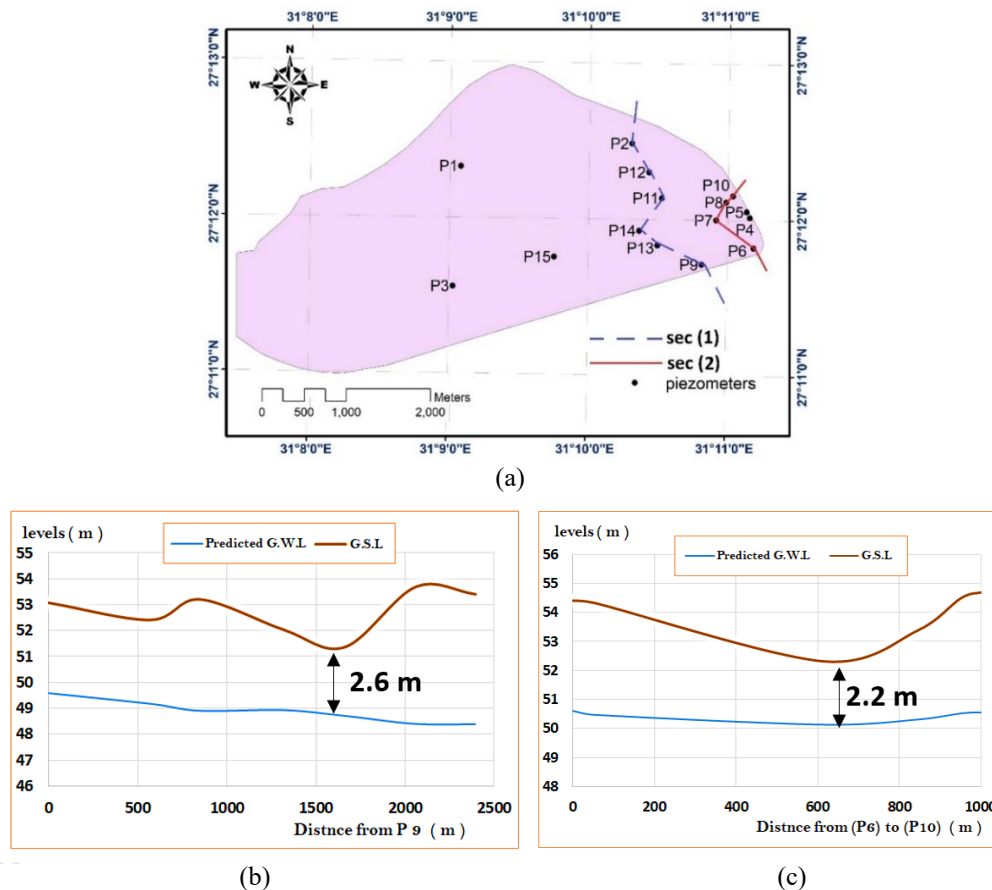


Fig. 12. (a) locations of sections, (b) sec (1), (c) sec (2).

Fig. 12 illustrates the relationship between ground levels and the predicted groundwater levels (GWL) after the operation of the New Assiut Barrage. The specific location referred to as "section (1,2)" falls within the Walidiyah district, an area characterized by a high population density and the presence of numerous structures. Situated upstream of the barrage, this region is particularly susceptible to issues arising from rising GWL following the NAB operation. Fig. 11 shows a notable increase in groundwater levels, which previously stood before NAB construction, at a minimum of 3.67 meters and 4.25 meters in these sections. However, post-operation, the GWL has risen to approximately 2.6 meters and 2.2 meters, reflecting an average increase of around 1.5 meters.

## 8 CONCLUSIONS

This study presents and discusses the spatial distribution prediction of the GWL due to NAB construction, using a FD model and GIS. The effect of this increase in water level after the construction of NAB on GWL changes in the area adjacent to the barrage is studied. GIS and FDM with modifications in the meshing method to improve the accuracy, to create a model for the flow of groundwater and boundary conditions in the study area. The results at the maximum operation case indicate that, the average increase of GWL with 1.5 m after the operation of the NAB, this increase does not cause any emergence of groundwater in internal area of the study area, but it increases the amount of immersion that occurs to the side adjacent to the Nile River, where the expected total length of the submerged part from banks is 4.25 km, with an area of 240 feddan, there is an average increase in the percentage of areas prone to immersion after the operation by 50% from before, and an average increase in the total length of the banks exposed to immersion by 48%. When comparing maps of the immersion areas with the maps of the distribution of residential blocks, there is no a visible effect on the existing residential buildings there, but there is an industrial area (was built and operation in 2018) will be exposed to immersion, when the case of the maximum GWL after the operation of NAB. There will be no emergence of groundwater in The Waleediyah district, but the increase of GWL affect the foundations of buildings and tunnels, and may lead to landslides, so must study this effect. There will be no emergence of groundwater in the agricultural areas near the al-Walidiyah channel in the central of study area, but the increase of GWL affects the root area of the plants, and may damage them later, so must study this effect. The importance of the obtained results from this study is to illustrate the effect of the construction and operation of new barrages on increasing the levels of groundwater in the surrounding area, to determine the extent of the damage that is occurring, and to give a scientific study to researchers in that field.

## ACKNOWLEDGMENTS

Our sincere thanks and appreciation to **Eng. Abdul Rahim Ahmed Ali**, (previous Director General of Environmental Studies for the New Assiut Barrage Project, Ministry of Irrigation), for his fruitful cooperation with us to reach these important results.

**REFERENCES**

- [1] Negm, A. M., Sakr, S., Abd-Elaty, I., & Abd-Elhamid, H. F. (2018). An Overview of Groundwater Resources in Nile Delta Aquifer. In *Groundwater in the Nile Delta* (pp. 3-44). Springer, Cham.
- [2] Pokrovsky, V. D., Dutova, E. M., Kuzevanov, K. I., Pokrovsky, D. S., & Nalivaiko, N. G. (2015). Hydrogeological Conditions Changes of Tomsk, Russia. In *IOP Conference Series: Earth and Environmental Science* (Vol. 27, No. 1, p. 012031). IOP Publishing.
- [3] Phi, T. H., & Strokova, L. A. (2015). Prediction maps of land subsidence caused by groundwater exploitation in Hanoi, Vietnam. *Resource-Efficient Technologies*, 1(2), 80-89.
- [4] Medovar, Y. A., Yushmanov, I. O., & Bronskaya, E. E. (2018). Changes in the Ecological Condition of a Territory at the Construction of Buildings with a Deep Foundation under Various Geological Conditions in Moscow. *Water Resources*, 45(2), 65-72.
- [5] Mohamed, N. N. (2017). Use of Groundwater in Nile Alluvial Soils and Their Fringes. In *Groundwater in the Nile Delta* (pp. 107-140). Springer, Cham.
- [6] Galluzzo, B. J. (2011). A finite-difference based approach to solving the subsurface fluid flow equation in heterogeneous media.
- [7] Xu, X., Huang, G., Qu, Z., & Pereira, L. S. (2011). Using MODFLOW and GIS to assess changes in groundwater dynamics in response to water saving measures in irrigation districts of the upper Yellow River basin. *Water resources management*, 25(8), 2035-2059.
- [8] Yang, Q., Lun, W., & Fang, Y. (2011). Numerical modeling of three dimension groundwater flow in Tongliao (China). *Procedia Engineering*, 24, 638-642.
- [9] Kumar, C. P., & Singh, S. (2015). Concepts and modeling of groundwater system. *Int. J. Innov. Res. Sci. Eng. Technol*, 2(2), 262-271.
- [10] Anderson, M. P., Woessner, W. W., & Hunt, R. J. (2015). *Applied groundwater modeling: simulation of flow and advective transport*. Academic press.
- [11] Jafari, F., Javadi, S., Golmohammadi, G., Karimi, N., & Mohammadi, K. (2016). Numerical simulation of groundwater flow and aquifer-system compaction using simulation and InSAR technique: Saveh basin, Iran. *Environmental Earth Sciences*, 75(9), 833.
- [12] Dawoud, M. A., El Arabi, N. E., Khater, A. R., & van Wonderen, J. (2006). Impact of rehabilitation of Assiut barrage, Nile River, on groundwater rise in urban areas. *Journal of African Earth Sciences*, 45(4-5), 395-407.

- [13] El-Tuhami, A., & Mohamed, H. I. (2008). Groundwater levels estimation at areas affected by new Naga Hammadi barrages using ANN method. In *Twelfth international water technology conference, Alexandria, Egypt*.
- [14] El-Fakharany, Z., & Fekry, A. (2014). Assessment of New Esna barrage impacts on groundwater and proposed measures. *Water Science*, 28(1), 65-73.
- [15] Abdalla, F., & Shamrukh, M. (2016). Quantification of River Nile/Quaternary aquifer exchanges via riverbank filtration by hydrochemical and biological indicators, Assiut, Egypt. *Journal of Earth System Science*, 125(8), 1697-1711.
- [16] Abdellatif, R., Ramadan, M. A., & Kamel, M. S. (2016). Groundwater Evaluation for Drinking and Domestic Uses in Diruot District, Assiut City, Egypt.
- [17] Noureldeen, A. S., Ghaly, S., Ali, K., & Abozaid, G. (2017, November). ANN-Based Approach to Predict Changes in Ground Water Levels as a Result of Constructing New Naga-Hammadi Barrage, Egypt. In *Euro-Mediterranean Conference for Environmental Integration* (pp. 853-856). Springer, Cham.
- [18] Krishnamurthy, J., Venkatesa Kumar, N., Jayaraman, V., & Manivel, M. (1996). An approach to demarcate ground water potential zones through remote sensing and a geographical information system. *International Journal of Remote Sensing*, 17(10), 1867-1884.
- [19] Laurent, F., Anker, W., & Graillet, D. (1998). Spatial modelling with geographic information systems for determination of water resources vulnerability application to an area in massif central (france) 1. *Jawra Journal of the American Water Resources Association*, 34(1), 123-134.
- [20] Watkins, D. W., McKinney, D. C., Maidment, D. R., & Lin, M. D. (1996). Use of geographic information systems in ground-water flow modeling. *Journal of Water Resources Planning and Management*, 122(2), 88-96.
- [21] Pinder, G. F. (2002). *Groundwater modeling using geographical information systems*. John Wiley & Sons.
- [22] Patra, H. P., Adhikari, S. K., & Kunar, S. (2016). Geophysical Prospecting for Groundwater. In *Groundwater Prospecting and Management* (pp. 53-134). Springer, Singapore.
- [23] Zdechlik, R. (2016). A review of applications for numerical groundwater flow modeling. *International Multidisciplinary Scientific GeoConference: SGEM*, 3, 11-18.
- [24] Igboekwe, M. U., & Achi, N. J. (2011). Finite difference method of modelling groundwater flow. *Journal of Water Resource and Protection*, 3(3), 192-198.

- [25] Casulli, V., & Cheng, R. T. (1992). Semi-implicit finite difference methods for three-dimensional shallow water flow. *International Journal for numerical methods in fluids*, 15(6), 629-648.
- [26] Chen, S. Y., Hsu, K. C., & Fan, C. M. (2021). Improvement of generalized finite difference method for stochastic subsurface flow modeling. *Journal of Computational Physics*, 429, 110002.
- [27] Wang, Y., Cui, Y., Shao, J., & Zhang, Q. (2019). Study on Optimal Allocation of Water Resources Based on Surrogate Model of Groundwater Numerical Simulation. *Water*, 11(4), 831.
- [28] Galluzzo, B. J. (2011). A finite-difference based approach to solving the subsurface fluid flow equation in heterogeneous media.
- [29] McDonald, M. G., & Harbaugh, A. W. (1988). *A modular three-dimensional finite-difference ground-water flow model*. US Geological Survey.
- [30] Neuman, S. P. (1973). Calibration of distributed parameter groundwater flow models viewed as a multiple-objective decision process under uncertainty. *Water Resources Research*, 9(4), 1006-1021.
- [31] Akhter, M. G., Ahmad, Z., & Khan, K. A. (2006). Excel based finite difference modeling of ground water flow. *Journal of Himalayan Earth Sciences*, 39, 49-53.
- [32] Thomas, J. W. (2013). *Numerical partial differential equations: finite difference methods* (Vol. 22). Springer Science & Business Media. ISBN: 978-1-4899-7278-1 (eBook).
- [33] El Tahlawi, M. R., Farrag, A. A., & Ahmed, S. S. (2008). Groundwater of Egypt: "an environmental overview". *Environmental Geology*, 55, 639-652.
- [34] Said R (1962) *The geology of Egypt*. Elsevier Pub. Comp, Amesterdam, New York, p 377
- [35] Abou El-Anwar, E. A., Mekky, H. S., Salman, S. A., Elnazer, A. A., Abdel Wahab, W., & Asmoay, A. S. (2019). Mineralogical and petrographical studies of agricultural soil, Assiut Governorate, Egypt. *Bulletin of the National Research Centre*, 43, 1-9.
- [36] Osman HZ (1980) *Geological studies on the area to the northwest of Assiut* M.Sc. thesis, Fac. Sci., Assiut Univ., Assiut, Egypt, p 276
- [37] Abdel-Mawgoud, A., & Faragallah, M. E. A. (2004). CHARACTERIZATION OF SOME NILE ALLUVIAL SOILS AT ASSIUT. EGYPT. *Journal of Soil Sciences and Agricultural Engineering*, 29(9), 5335-5346.
- [38] Conoco, *Geologic map of Egypt* (1987) Egyptian general authority for petroleum. NG 36 NW Asyut
- [39] Modified image from Google Earth Pro. Software.